# SQUID readout and ultra-low magnetic fields for Gravity Probe-B (GP-B)

James M. Lockhart

GP-B Program, Stanford U., and Physics Dept., San Francisco State U.
Hansen Laboratories, Stanford, California 94305

## Abstract

We describe the superconducting readout system to be used for resolving 0.001 arc second changes in the gyroscope spin direction in the Relativity Gyroscope (GP-B) experiment. This system couples the London magnetic moment flux of the spinning gyro to a low noise superconducting quantum interference device (SQUID) detector. Resolution limits and noise performance of the detection system will be discussed, and improvements obtained and expected with advanced SQUIDs will be presented. We also describe the novel use of superconducting magnetic shielding techniques to obtain a 250 dB attenuation of the Earth's magnetic field at the location of the gyroscopes. In this approach, expanded superconducting foil shields (as developed by Cabrera[1]) are coupled with fixed cylindrical superconducting shields and special geometric considerations to obtain the extremely high attenuation factor required. With these shielding techniques, it appears that the 0.5 Gauss Earth field (which appears to the gyroscopes as an AC field at the satellite roll rate) can be reduced to the $10^{-13}$ G level required by the experiment. We present recent results concerning improvements in the performance of the superconducting foil technique obtained with the use of a new computer-controlled cooling system.

## Introduction

An earlier paper in this conference (Bardas, et al.) has described the Gravity Probe-B Relativity Gyroscope experiment. In this paper we describe in some detail the superconducting readout system used for resolving 0.001 arc second changes in the gyroscope spin direction and the novel use of superconducting magnetic shielding techniques to obtain the extremely low background magnetic fields required by the readout system. The sensitivity and resolution required in the readout system place very severe demands on detector technology, particularly with regard to linearity and 1/f noise limits. The extremely high performance required of the readout system in turn places two very stringent requirements on the magnetic shielding needed in the experiment. The solutions to these problems represent a very interesting coupling of fundamental science with technology.

## Principles of the superconducting gyroscope readout

The physical basis of the superconducting readout, shown in Fig. 1, is the London magnetic moment which develops in a rotating superconducting body which is spun up after being cooled to a temperature below its superconducting transition point. The effects of this magnetic moment are externally equivalent to those of a magnetic field which is uniform inside the rotor, is exactly aligned with the spin axis, and is of magnitude

$$B_L = -(2mc/e)\omega_s = 1.14 \times 10^{-7}\ \omega_s \text{ Gauss} \qquad (1)$$

where $\omega_s$ is the spin angular velocity, m and e are the electron mass and charge, and c is the velocity of light. In SI units, and in terms of the rotation frequency f, this field is

$$B_L = 7.15 \times 10^{-11}\ f \text{ Tesla.} \qquad (2)$$

In the case of the GP-B program, the gyroscope rotor is the spinning body and the rotation frequency f has the baseline value of 170 Hz, so the London moment field amounts to $1.22 \times 10^{-8}$ Tesla. The readout system is required to detect changes in the direction of this field to a precision of 0.001 arc second.

As described in the earlier paper, the gyroscope rotor is electrostatically suspended in a housing. The housing contains a thin film superconducting pickup loop placed on the parting plane so as to form a great circle around the rotor. This loop serves to couple the London moment flux from the rotor to a flux-to-voltage converter known as a SQUID (Superconducting Quantum Interference Device), as shown in Fig. 1. For clarity, the figure shows only a single-turn pickup loop (of inductance $L_R$) instead of the multi-turn pickup loop which we plan to use in the actual experiment. The figure also shows the stray inductance $L_{stray}$ in the leads connecting the pickup loop to the SQUID as well as the inductance $L_S$ associated with the input coil of the SQUID.

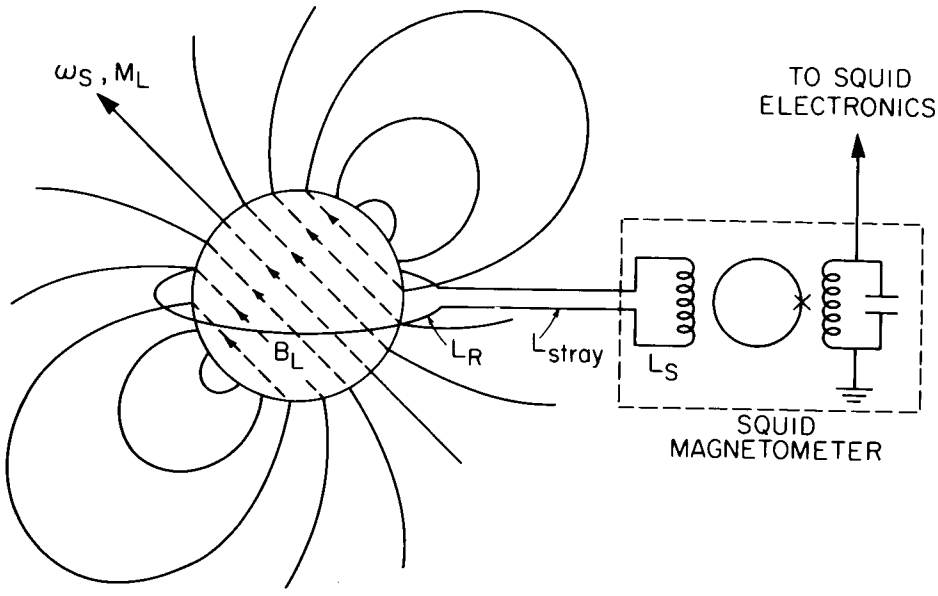


Fig. 1: Superconducting gyro readout

As the spin axis of the gyroscope changes direction, the flux intercepted by the pickup coil will change in proportion. Since the gyroscope spin is initially aligned to be almost exactly in the plane of the pickup loop, the flux intercepted by a loop having a radius only infinitesimally larger than the rotor radius $r_r$ will be given by

$$\Phi = N^* B_L \pi r_r^2 \sin\theta \tag{3}$$

where $\theta$ is the angle the spin vector makes with the plane of the pickup loop and $N^*$ is the effective number of turns in the loop, taking into account the departure from perfect flux coupling in a multi-turn loop. Since $\theta << 1$, we can take $\sin\theta \sim \theta$.

We now consider how much of the change in flux resulting from a change of the gyroscope spin angle from $\theta_0$ to $\theta_1$ will actually appear at the flux-voltage converter. The pickup loop forms part of a closed superconducting circuit and the total flux enclosed by this circuit will remain constant as long as the loop is kept below the superconducting transition temperature (as required by the electrodynamics of superconductors). A change in the flux intercepted by the loop will induce a current in the loop circuit which will act to keep the total flux constant. In terms of the inductances $L_R$, $L_S$, and $L_{stray}$ as illustrated in Fig. 1, the current will be of magnitude

$$I_R = \Phi / (L_R + L_S + L_{stray}). \tag{4}$$

We will consider $L_{stray} << L_R$, $L_S$ and drop it. The energy delivered to the input coil of the flux-voltage converter (SQUID) is thus

$$E_S = 0.5\, L_S I_R^2 = 0.5\, L_S [\Phi / (L_R + L_S)]^2. \tag{5}$$

Clearly this energy is maximized by maximizing $\Phi$ while minimizing $L_R$ and then selecting the matching condition $L_R = L_S$. From the value of this coupled energy, the transfer function of the SQUID, and the SQUID noise levels, we can compute the overall sensitivity of the readout system.

We have recently devoted considerable attention to the simultaneous maximization of $\Phi$ and minimization of $L_R$ in multi-turn pickup loops. With a "compact" multi-turn coil (one in which the windings fill a minimum volume), we have $\Phi = k_1 N$ and $L_R = k_2 N^2$. Then assuming matching $(L_R = L_S)$, we have

$$\begin{aligned} E_S &= 0.5\, L_R [\Phi / (L_R + L_S)]^2 \\ &= 0.5\, k_2 N^2 [k_1 N / 2k_2 N^2]^2 \\ &= 0.125\, k_1^2 / k_2 \end{aligned} \tag{6}$$

and we see that there is no advantage to the multi-turn loop. However, it is possible to construct the pickup coil so as to make its self-inductance increase less rapidly with N

than $N^2$ while retaining or only slightly reducing the linear dependence of the captured flux on N. We see three ways to accomplish this:

1) space the turns away from each other in the radial dimension in such a way as to optimize the ratio $\Phi^2 / L_R$

2) use a superconducting ground plane below the pickup loop (this reduces the inductance in general as well as reducing the dependence on N)

3) place "guard rings" of superconductor between windings to reduce the mutual inductance of the various turns.

By combining 1), 2), and 3), it appears that a significant increase can be achieved in the energy delivered to the SQUID sensor. For example, the plot of Fig. 2 shows the "figure of merit" $(\Phi^2 / L_R)$ which can be achieved by choosing optimal spacing of the individual turns in a multi-turn loop. Fig. 3 shows a view of a five-turn pickup loop geometry based on these considerations. Adding a ground plane and guard rings would appear to allow a reduction by a factor of perhaps as much as 5 in the total self-inductance, thus allowing a corresponding increase in the figure of merit.

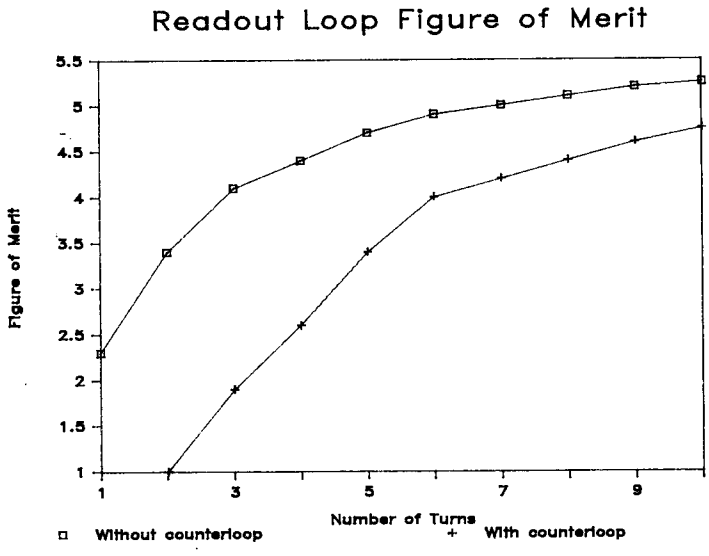


Fig. 2: Figure of merit for multi-turn loops.

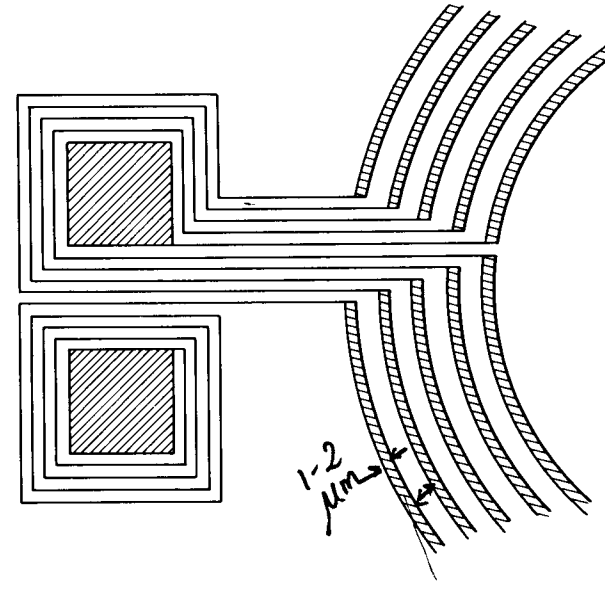


DETAIL OF CONTACT PAD AREA

Fig. 3: Pickup loop arrangement

Once the flux signal is delivered to the SQUID, it is parametrically converted by the action of the SQUID device to an easily measured voltage. Resolution is limited at that point by

1) noise contributed by the SQUID system, and

2) interference signals picked up in the input circuit.

In the case of SQUID noise, we are helped tremendously by satellite roll. With roll, the angular displacement of the gyro spin axis from the plane of the pickup loop caused by the geodetic and motional effects results in a sinusoidally varying pickup flux at the satellite roll frequency with the amplitude of the sine wave proportional to the relativity signal. It is thus possible to "narrow band" around the signal frequency to reduce the effective noise bandwidth. We will discuss this point at greater length below. The question of interfering signals dictates the stringent magnetic shielding requirements mentioned earlier.

A SQUID constitutes the lowest-noise amplifier system known; however, like all detector systems, it exhibits both white noise and 1/f noise. A typical set of SQUID noise power spectral density plots is shown in Fig. 4, which also shows the signal frequency corresponding to the baseline 10 minute roll period. The data of the top curve is characteristic of the RF-biased SQUIDs which we have used for several years; it predicts a noise power spectral density of about $6.8 \times 10^{-27}$ J/Hz at the signal frequency. The SQUID output must be synchronously demodulated to recover the roll-frequency component and then integrated (i.e., low pass filtered) to give an effective noise bandwidth such that the noise energy in the measurement bandwidth is less than the signal energy corresponding to the resolution required; for the above numbers this implies an integration time of nearly 700 hours for a

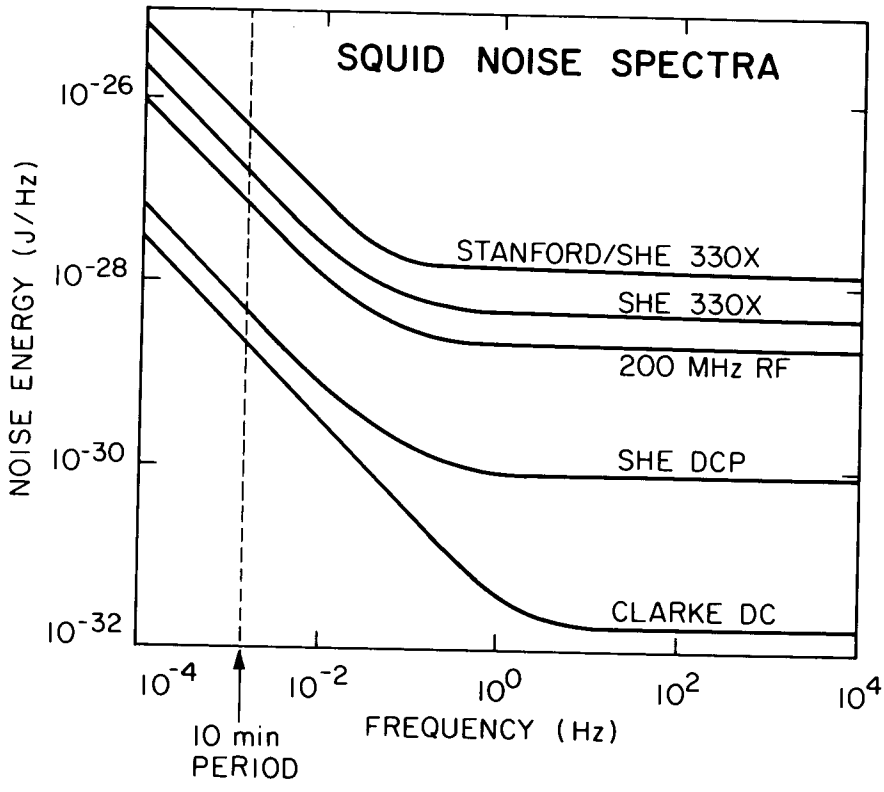


Fig. 4: Noise power spectral density for several SQUIDs

resolution of one milliarcsecond. While this integration time is feasible, it is undesirable for several reasons. It increases certain stability requirements in other parts of the measurement system as well as limiting the precision with which the geodetic and motional coefficients can be determined in a 1-2 year mission. We project that advances currently being incorporated into the readout system will give us an immediate improvement sufficient to reduce the integration time to about 70 hours for one milliarcsecond resolution. We anticipate that further advances to be discussed below are likely to reduce the integration time to something less than 10 hours.

Incorporation of the superconducting guard rings and ground plane into the readout loop should easily give us a factor of 3-4 net increase in signal energy delivered to the SQUID for a one milliarcsecond gyro angle displacement. Recent experiments in our laboratory with RF SQUIDs operated at a 200 MHz bias frequency with control electronics newly developed by Quantum Design Corp. have shown an effective reduction in the SQUID noise energy at our signal frequency by a factor of 3-4. While we have yet to demonstrate that these two improvement factors will be maintained when the new loop design is coupled to the 200 MHz SQUID, we have no reason to suspect any reduction. We should thus expect a factor of about ten improvement in minimum detectable energy, thus allowing the 70 hour integration time referred to above.

We hope that newer DC SQUID systems with even lower noise figures can be adapted to our readout system. Fig. 4 shows the noise properties of several advanced DC SQUIDs. We have already begun exploring the use of DC SQUIDs of the Clarke type in our work. High performance SQUIDs with designs similar to that of Clarke have recently been fabricated at IBM Research Labs., Yorktown Heights, and at the National Bureau of Standards, Boulder. If the noise figures which have been measured with the bare (i.e., shorted input) IBM SQUIDs could be maintained when the SQUIDS are incorporated in a measurement system, then coupling these SQUIDs with modest pickup loop improvements could potentially reduce the integration time to as little as 2 hours, allowing considerable improvement in the experiment. Fig. 5 shows the effect of reductions in SQUID noise on the uncertainty in the determination of the motional coefficient for a one year mission with a September launch date. This figure, which comes from the work of R. Vassar[2], must be adjusted somewhat for the fact that we now plan to use only one pickup loop per gyro rather than the two assumed by Vassar. However, the potential improvement is easy to see. By combining the very best of current DC SQUID device technology with appropriate work in the areas of reliability, packaging, and protection, and by adding the readout loop improvements which we have discussed, we might be able to do as well as the 1/16 SQUID noise amplitude factor shown; perhaps, with everything in

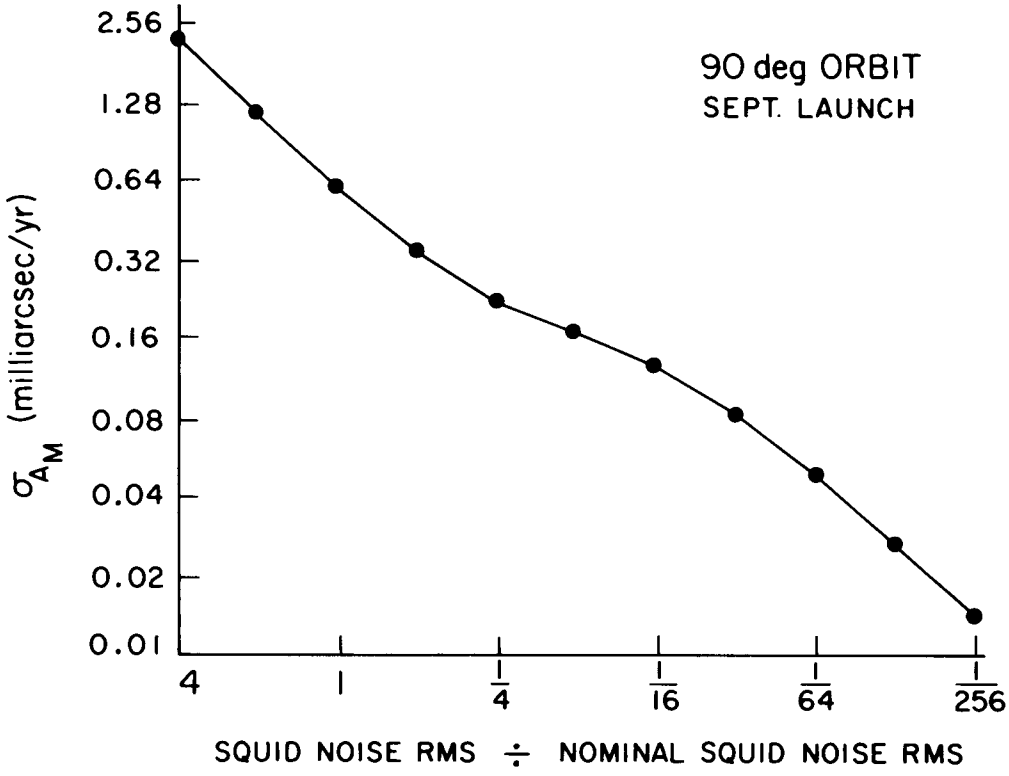


Fig. 5: Motional coefficient uncertainty vs. SQUID noise

our favor, even as well as the 1/64 figure. Of course, as SQUID noise levels are reduced to such small values, other error sources will become dominant (this effect is not considered in Fig. 5). In any event, there is much to be gained from the integration of low noise DC SQUIDs into our readout system.

In order to achieve any of these high resolution readout systems, including our baseline system, extreme care must be taken in implementing the detection system. The SQUIDs must be temperature controlled to better than 100 μK, great care must be taken in grounding and shielding, and dynamic range problems caused by trapped flux in the rotor and by pickup of interference from high level suspension signals must be dealt with. The readout loop must be positioned to within 0.5 mil of the rotor center, and the current distribution in the loop must be maintained constant to within a few Angstroms. Other effects which are negligibly small in practically all other detection systems become significant at the extreme sensitivity which we employ. An example is the problem of equivalent flux noise generated by circulating currents due to the Thomson effect in any normal metal in the vicinity of the pickup loops. The Thomson effect is the phenomenon of thermoelectric current generation in metals subject to a temperature gradient. This effect requires that only metals having a high ratio of electrical resistivity to thermal resistivity be used in the vicinity of the gyros unless heat flows in the quartz block area can be managed in such a way as to keep thermal gradients to very small levels. Tests with the London Moment Apparatus in our laboratory have shown that it is possible to control these effects to obtain good readout resolution. Further work as part of the First Integrated Systems Test (FIST) will allow investigation of these effects with an even more sensitive readout system.

## Superconducting magnetic shielding

In addition to the requirement for low SQUID noise, we mentioned the need for extreme levels of magnetic shielding. Very low DC background magnetic fields are required at the gyro position in order to avoid the trapping of excessive amounts of magnetic flux in the gyro rotor when it goes superconducting. SQUID dynamic range limitations dictate that the trapped flux in the rotor must correspond to a residual field of less than $10^{-7}$ G.

There is also the requirement that any magnetic signals at the roll rate which could be seen by the pickup loop should be less than an amount corresponding to the desired 0.001 arc sec resolution. Since the 0.6 G magnetic field of the Earth appears to the pickup to have a component varying at the satellite roll rate, this ac magnetic field must be shielded; in fact, sufficient shielding is required to obtain approximately 13 orders of magnitude attenuation of this field before it reaches the gyro location.

This shielding is accomplished through a six-component strategy which relies heavily on the use of superconductivity. Starting from the outside of the dewar and working our way to the pickup loop, we first have a conventional single layer cylindrical mu-metal magnetic shield which provides both DC and AC shielding (note that any mechanism which provides DC shielding will also provide AC shielding, although the converse is not true). The next level of shielding is provided by an open cylinder of expanded superconducting foil, often referred to as the "lead bag" due to the material of its construction.

The mechanically expanded superconducting foil technique was developed principally by Cabrera[1]. Fig. 6 illustrates the process by which a low residual magnetic field is attained.

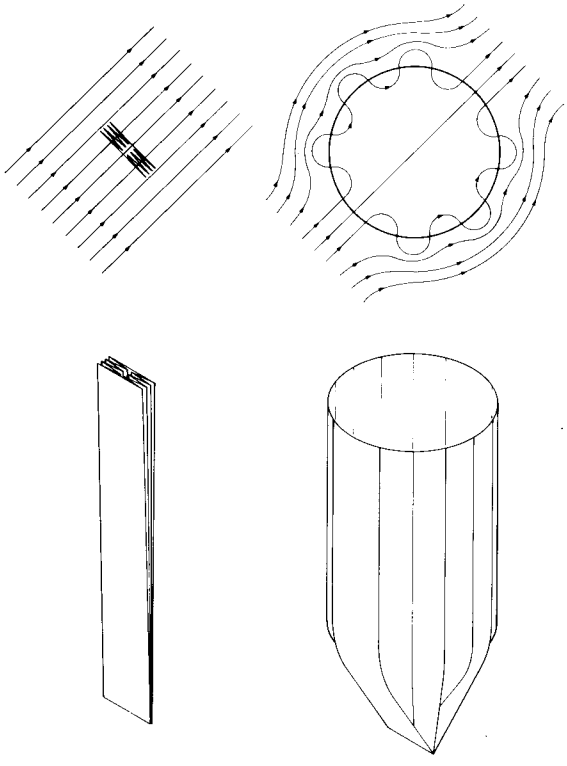

Fig. 6: Principle of superconducting foil shield

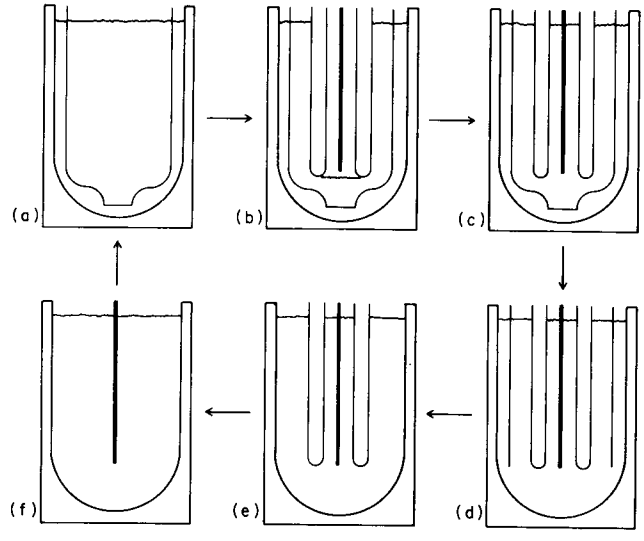


Fig. 7: Cooling and expansion cycle

The process depends on the fact that the total magnetic flux enclosed by a superconducting loop is conserved. Another phenomenon of superconductivity, the Meissner effect, predicts total expulsion of magnetic flux from a superconductor; this would theoretically permit the reduction of field in the shield cylinder to an amount set by flux penetration through the open end of the cylinder. However, the true Meissner effect only occurs in very pure single crystals of superconductor. A large superconducting object like the folded foil shield shown in the left half of Fig. 6 will have flux lines entering the material at several different locations, as illustrated. The flux lines tend to stay anchored, or pinned, to these sites. If the folded shield is now mechanically unfolded, or expanded, while being maintained at a temperature below the superconducting transition, the flux through the shield will stay constant, but because of the large increase in area the magnetic field (flux per unit area) will decrease in inverse proportion. The expansion process has thus reduced the residual field. We can now repeat the cycle, as illustrated in Fig. 7. We insert a new folded foil shield inside the existing expanded shield (a,b), then (b,c) cool the new shield to a temperature below the superconducting transition, and next (c) break a thin membrane seal at the bottom of the vacuum cooling tube and allow the liquid helium to rise in the tube. We then (d) slice out the bottom of the old shield, remove the old shield (e), and then expand the new shield after removing the old one (f,a). Since the second expansion takes place in a region of reduced residual field, less flux will be trapped and an even smaller background field will result after the second expansion. We typically go through the sequence 4-5 times to obtain a background field of less than $10^{-7}$ G.

The performance of the expanded foil technique is limited by thermomagnetic effects in the superconducting material. As the foil cools, temperature gradients generate thermoelectric potential differences which in turn generate electrical currents. These currents can be quite large because of the rather low normal state resistance of the superconducting material at temperatures just above the superconducting transition. These circulating

currents generate magnetic flux which is trapped as sections of the material drop below the transition temperature.

Reduction of background fields to levels of $10^{-5}$ G and below requires special cooling procedures in order to avoid the limitations set by the thermomagnetic effects. The optimum procedure seems to be one in which the shield is cooled at a very slow rate with the entire shield structure maintained as isothermal as possible, i.e., with the cooling arranged to minimize spatial variations in temperature.

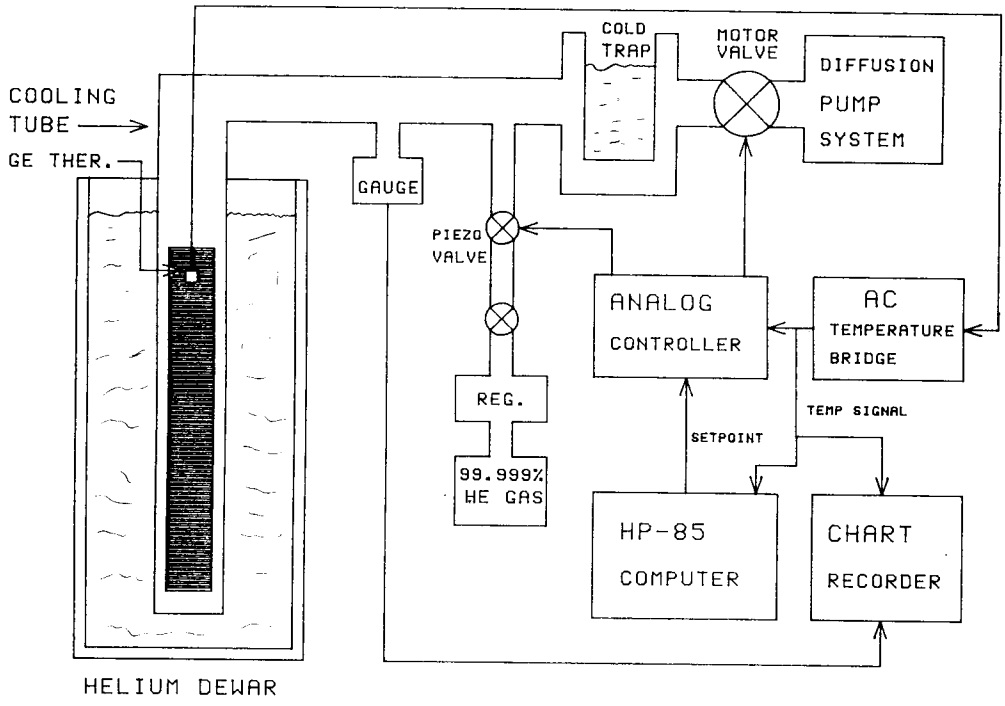


Fig. 8: Cooling system for lead bag

The system we utilize for shield cooling is shown in Fig. 8. The shield is placed inside a glass vacuum tube which is pumped down to a vacuum of $10^{-6}$ Torr or better. The tube is then placed in the helium dewar and a small amount of He exchange gas is admitted to the tube to start the cooling process. The cooling rate is regulated by a feedback control system which incorporates an HP-85 microcomputer. The exchange gas is admitted through a piezoelectric valve; its pressure is monitored by a capacitance manometer. A high vacuum pumping station (modified Veeco MS-17 leak detector) is also connected to the cooling tube. A motorized valve in the pump station permits the pumping speed to be electronically controlled. A Ge resistance thermometer is thermally anchored to the lead foil of the shield; it is read out with a low frequency ac bridge using phase sensitive detection.

Cooling proceeds as follows: a temperature setpoint is selected by the computer and sent to an analog controller, where it is compared with the output of the temperature bridge. The error signal is used to drive the pump throttle valve and/or the gas feed valve. The analog controller then continues to adjust the gas flow and pumping speed so as to maintain the setpoint. When temperatures near the superconducting transition are reached, the computer issues a setpoint, waits til the setpoint is attained, and then issues a new setpoint very slightly lower in temperature. In this way, any desired cooling profile can be achieved through the critical transition temperature region. In a typical cooling, a temperature drop of two Kelvin through the transition would be spread over a 15-20 hour period. Note that it is important here that the cooling be monotonic; oscillations of even a few tenths of a degree can cause thermomagnetic problems. Fig. 9 shows the cooling profile obtained in a recent run with the new cooling system. Note particularly that the rate of temperature drop is very slow in the region near the superconducting transition temperature of lead, which is shown as a dashed line in the figure. A final lead bag shield recently produced with this cooling technique yielded a background field of less than $9 \times 10^{-8}$ G in the gyro region.

The mu-metal and lead bag system together give a DC background field of less than $10^{-7}$ G (thus meeting the DC requirement), and an attenuation factor of about $2 \times 10^{-9}$ for ac fields applied transverse to the shield axis (the most difficult to shield). Further ac shielding is obtained in several ways. Each gyro is surrounded by a cylindrical

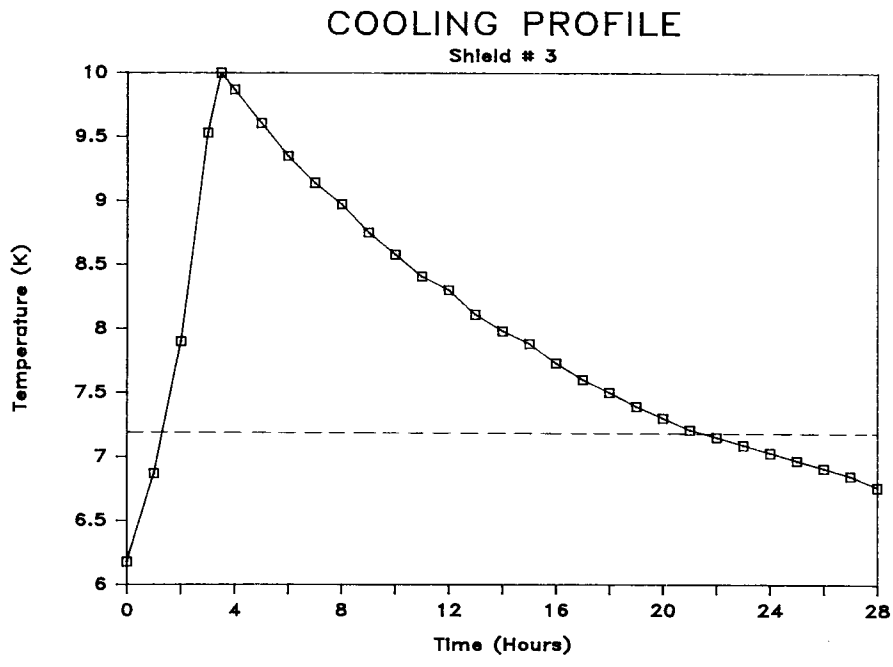


Fig. 9: Temperature profile during a shield cooling

superconducting shield which provides a minimum attenuation factor of about $10^{-2}$ as well as providing magnetic isolation of one gyro assembly from another. Another shielding factor is obtained by positioning the pickup coil so as to capitalize on the symmetry properties of the leakage fields in the shield. The rotor itself, being coated with superconductor, screens its area from ac pickup. Finally, the superconducting ground plane mentioned earlier aids in shielding the pickup loop from external flux. There is also the possibility of using a "counterwound coil" - a pickup coil wound as a radial gradiometer and thus capable of rejecting part of the external flux coupling. Table 1 shows the amount of shielding provided by each of these mechanisms.

Table 1: Attenuation of DC and AC Magnetic Fields

| Technique | DC Residual Field | AC Shielding Factor |
|---|---|---|
| Mu-metal shield | $3 \times 10^{-4}$ G | $5 \times 10^{-2}$ |
| Lead bag | $7 \times 10^{-8}$ G | $4 \times 10^{-7}$ |
| Local Gyro shield | | |
| (Direct) | - | $1 \times 10^{-2}$ |
| (Symmetry factor) | - | $3 \times 10^{-2}$ |
| Rotor self-shielding | - | $1 \times 10^{-1}$ |
| Ground plane/Counterloop | | $1\text{-}3 \times 10^{-1}$ |
| TOTAL | $7 \times 10^{-8}$ | $6\text{-}18 \times 10^{-14}$ |
| REQUIREMENT | $1 \times 10^{-7}$ | $2 \times 10^{-13}$ |

Residual fields in the superconducting shields are measured with either a SQUID-based flipcoil magnetometer which, with some repositioning for each vector measurement, allows the remanent field to be measured along the shield axis, or with a three-axis, SQUID-based residual field scanner.

## Summary

Through the use of computer modelling correlated with measurements on actual shielding structures, it has been possible to design an integrated readout and magnetic shielding system which will allow milliarcsecond resolution measurements of changes in the gyroscope spin direction in the GP-B program. Essentially all components of the system have been fabricated and tested in prototype versions. Thin film superconducting pickup loops have been fabricated by Dr. P. Peters at the NASA Marshall Space Flight Center and are now being tested. (We expect to begin fabricating loops in our own laboratory in the next few months, either by the UV direct write photolithography technique developed at Marshall Center or by

a newer technique of precision laser milling. These techniques were briefly described in the earlier paper of Bardas et al. SQUID readout systems with the baseline noise performance have been operated here for several years, and more recently newer SQUID systems with lower noise have been utilized (in particular the 200 MHz RF SQUID). Prototype local superconducting shields have been fabricated and tested. Lead bag shield systems having residual field performance in excess of the requirements have been produced. We have also worked with personnel from Lockheed Missiles and Space Corp. to transfer the superconducting foil shielding technology to them; they will be providing these shields for the FIST and STORE programs as well as the Science Mission. The calculations of shielding due to residual field symmetries have been experimentally verified.

In order for the output of the readout system which we have described to be useful, the SQUID voltage must be filtered, demodulated with respect to the satellite roll rate reference, and then combined with data from the telescope in order to yield the data on the geodetic and motional coefficients. These tasks are carried out by the elegant Science Data Instrumentation System devised by R. A. Van Patten. The functioning of this sytem and the results of a complete computer simulation of the entire signal processing system are discussed in the following paper by Van Patten, DiEsposti, and Breakwell. Their simulation includes the effects of 1/f noise in the SQUIDs as well as other uncertainties; it shows in a very interesting way the development in time of the estimates of the relativity coefficients.

We are now preparing several integrated readout system tests in which all of the readout and shielding components will be tested while working together as a complete system. At the same time, we are pursuing the use of advanced SQUIDs and expect to be able to reduce the required integration time by a factor of 10 to 50 , thus allowing achievement of a resolution in the gyroscope angle measurement of perhaps something less than 0.5 milliarcsecond. Many of these concepts will be further evaluated in the FIST program, especially the questions of total system performance with all of the various technologies combined. We look forward eagerly to still further tests of this system on the 1990 Space Shuttle flight.

## Acknowledgements

It is a pleasure to thank Chuck Warren, Dan Levin, Kingman Yee, and Anne Heavey for help with apparatus and measurements. Blas Cabrera contributed many useful discussions as well as the loan of items of equipment. Thanks is also due all the members of the Stanford GP-B program for various forms of support. The GP-B program is supported by NASA through the Marshall Space Flight Center.

## References

1. Cabrera, B., Ph.D. Thesis, Stanford University, 1975. Also Cabrera, B., and van Kann, F., Acta Astronautica 5, 125, 1978.
2. Vassar, R., Ph.D. Thesis, Stanford University, 1982.